

Synthesis of MoS_{2(1-x)}Se_{2x} and WS_{2(1-x)}Se_{2x} alloy for enhanced hydrogen evolution reaction performance

*Sajjad Hussain^{a,b}, Kamran Akbar^{a,c}, Dhanasekaran Vikraman^d, K. Karuppasamy^d, Hyun-Seok Kim^d, Seung-Hyun Chun^{a,c}, and Jongwan Jung^{*a,b}*

^aGraphene Research Institute, Sejong University, Seoul 05006, Republic of Korea

^bInstitute of Nano and Advanced Materials Engineering, Sejong University, Seoul 05006, Republic of Korea

^cDepartment of Physics, Sejong University, Seoul 05006, Republic of Korea.

^dDivision of Electronics and Electrical Engineering, Dongguk University-Seoul, Seoul 04620, Republic of Korea

* Corresponding author, E-mail: jwjung@sejong.ac.kr

Table S1. Comparison of electrochemical parameters for different electrocatalysts by using Pt as counter electrode.

Sample	Overpotential (mV vs RHE)	Tafel slope (mV·decade⁻¹)	Exchange current Density (j_o, mA·cm⁻²) @ 10 mA·cm⁻²
Pt	40	52	3.01
MoS₂	252	87	1.23 x 10 ⁻²
MoS_{2(1-x)Se_{2x}}	141	79	2.04 x 10 ⁻¹
WS₂	283	134	6.36 x 10 ⁻²
WS_{2(1-x)Se_{2x}}	167	108	2.63 x 10 ⁻¹

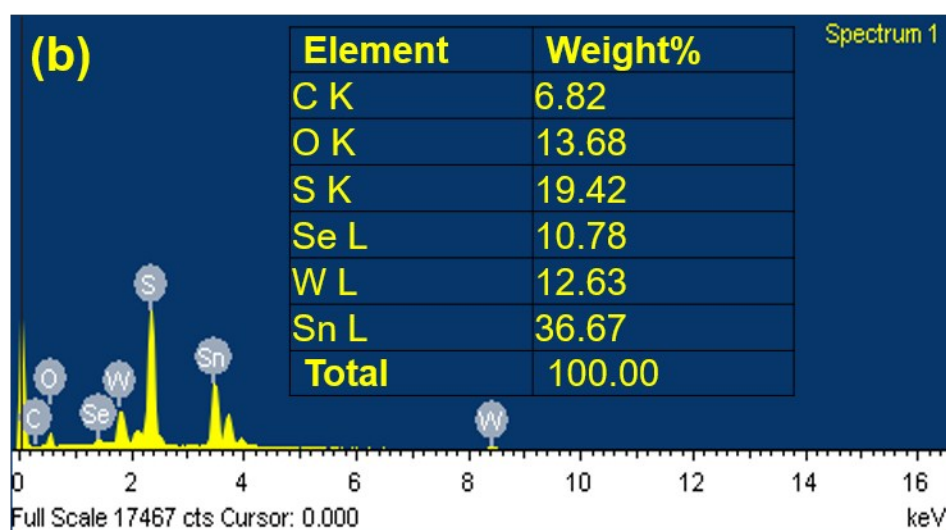
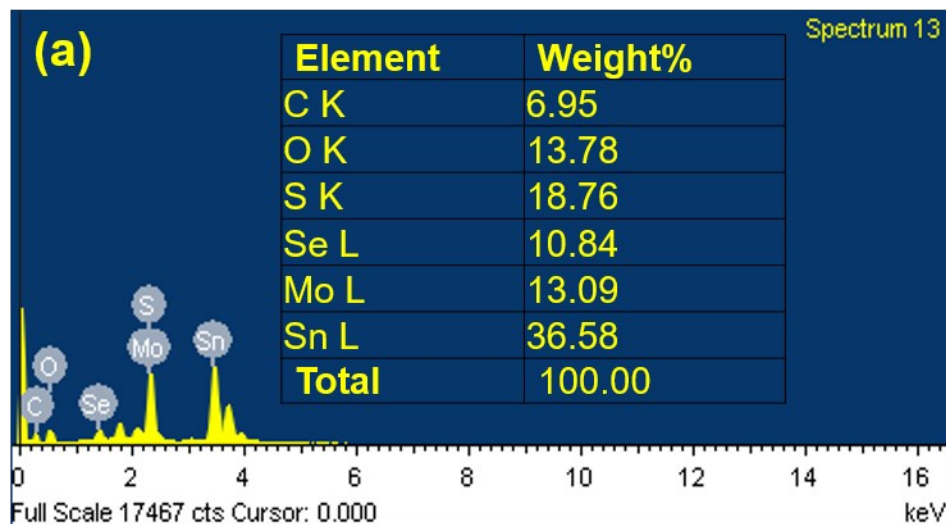


Figure S1 (a-b). EDS spectra of elemental composition for (a) $\text{MoS}_{2(1-x)}\text{Se}_{2x}$ and (b) $\text{WS}_{2(1-x)}\text{Se}_{2x}$ alloys.

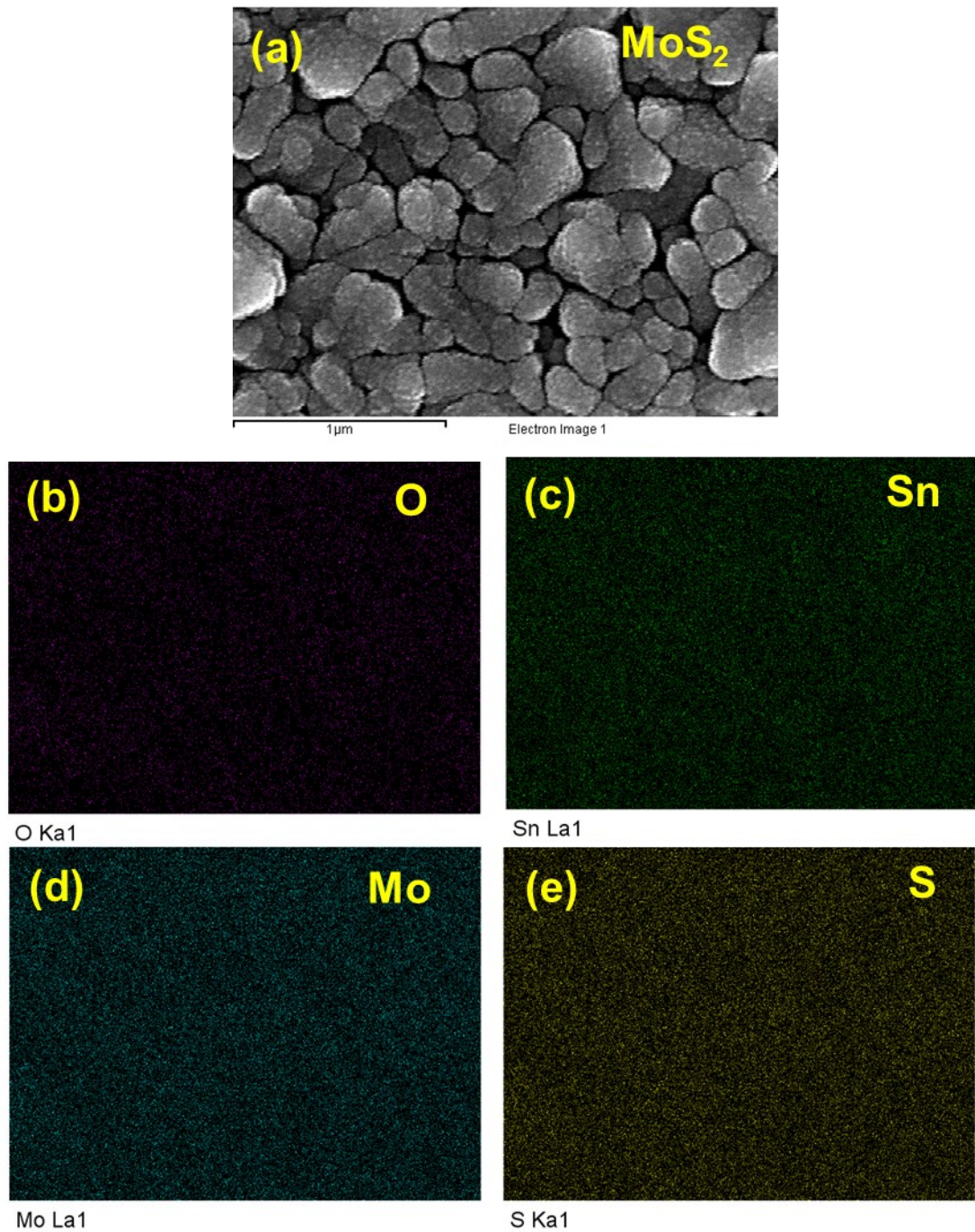


Figure S2. (a) FESEM image of MoS_2 and (b-e) their elemental mapping images (b) O (c) Sn (d) Mo and (e) S elements.

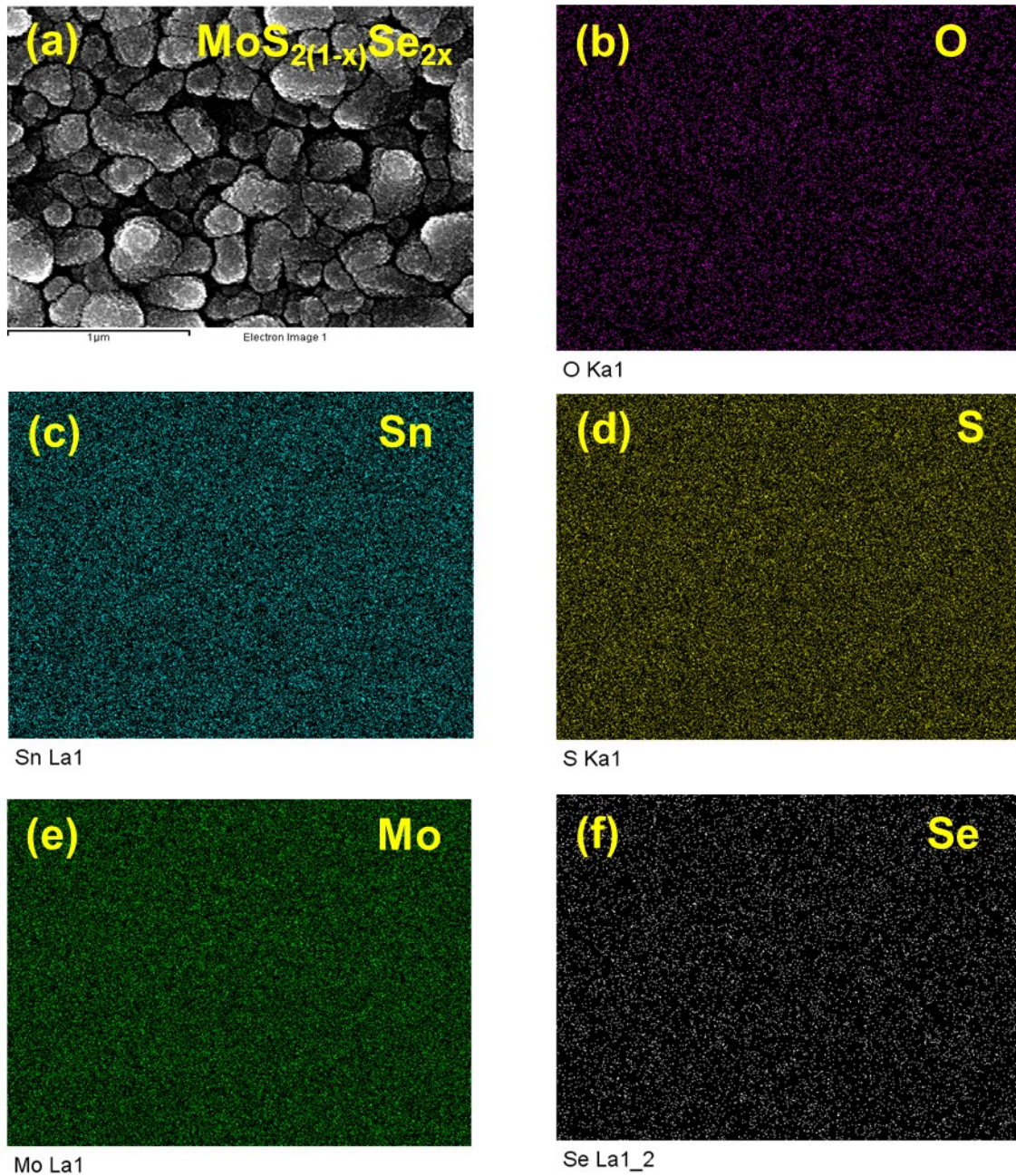


Figure S3. **(a)** FESEM image of $\text{MoS}_{2(1-x)}\text{Se}_{2x}$ alloy and **(b-f)** their elemental mapping images **(b)** O, **(c)** Sn, **(d)** S, **(e)** Mo and **(f)** Se elements.

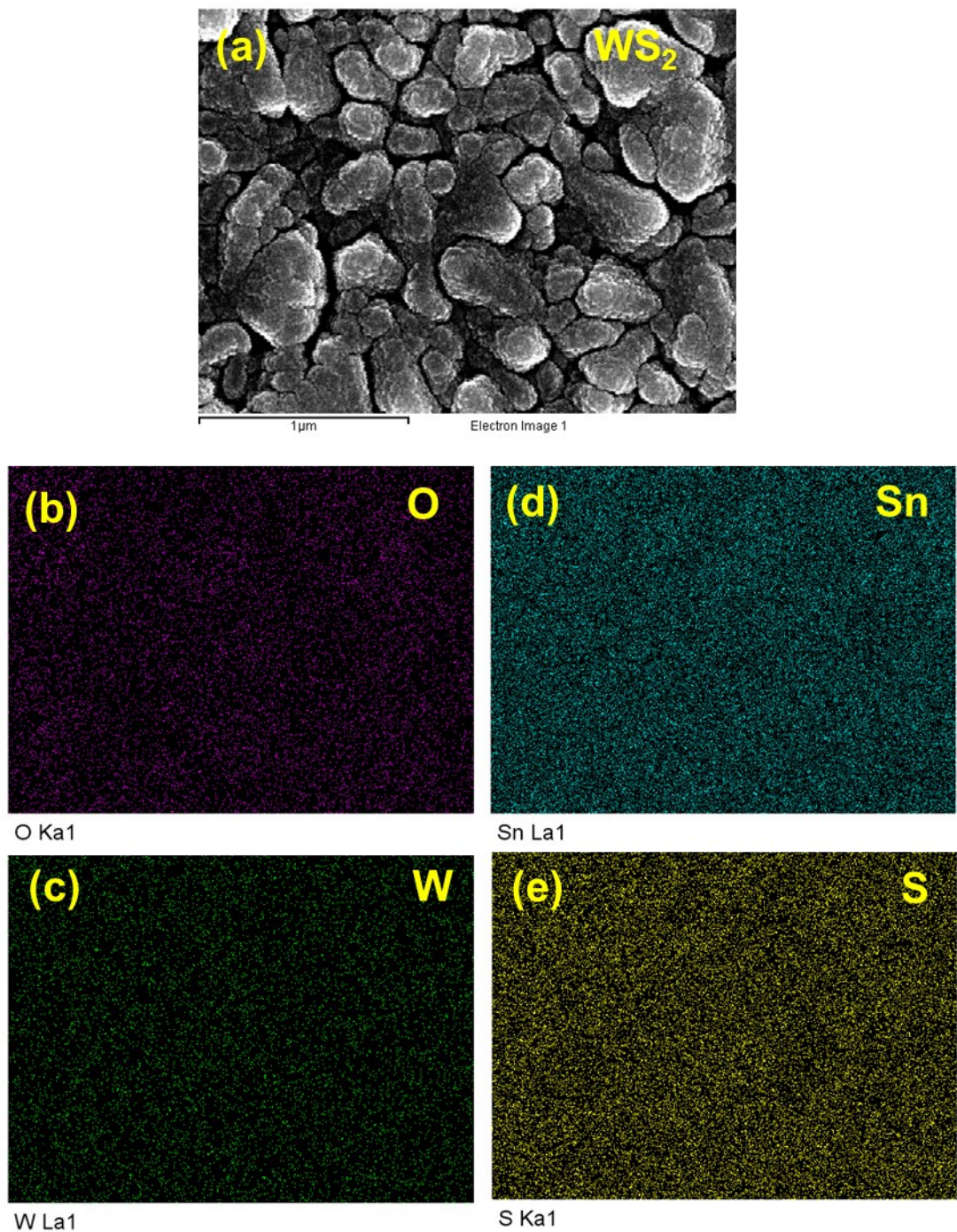


Figure S4. (a) FESEM image of WS_2 and (b-e) their elemental mapping images (b) O (c) Sn (d) W and (e) S elements.

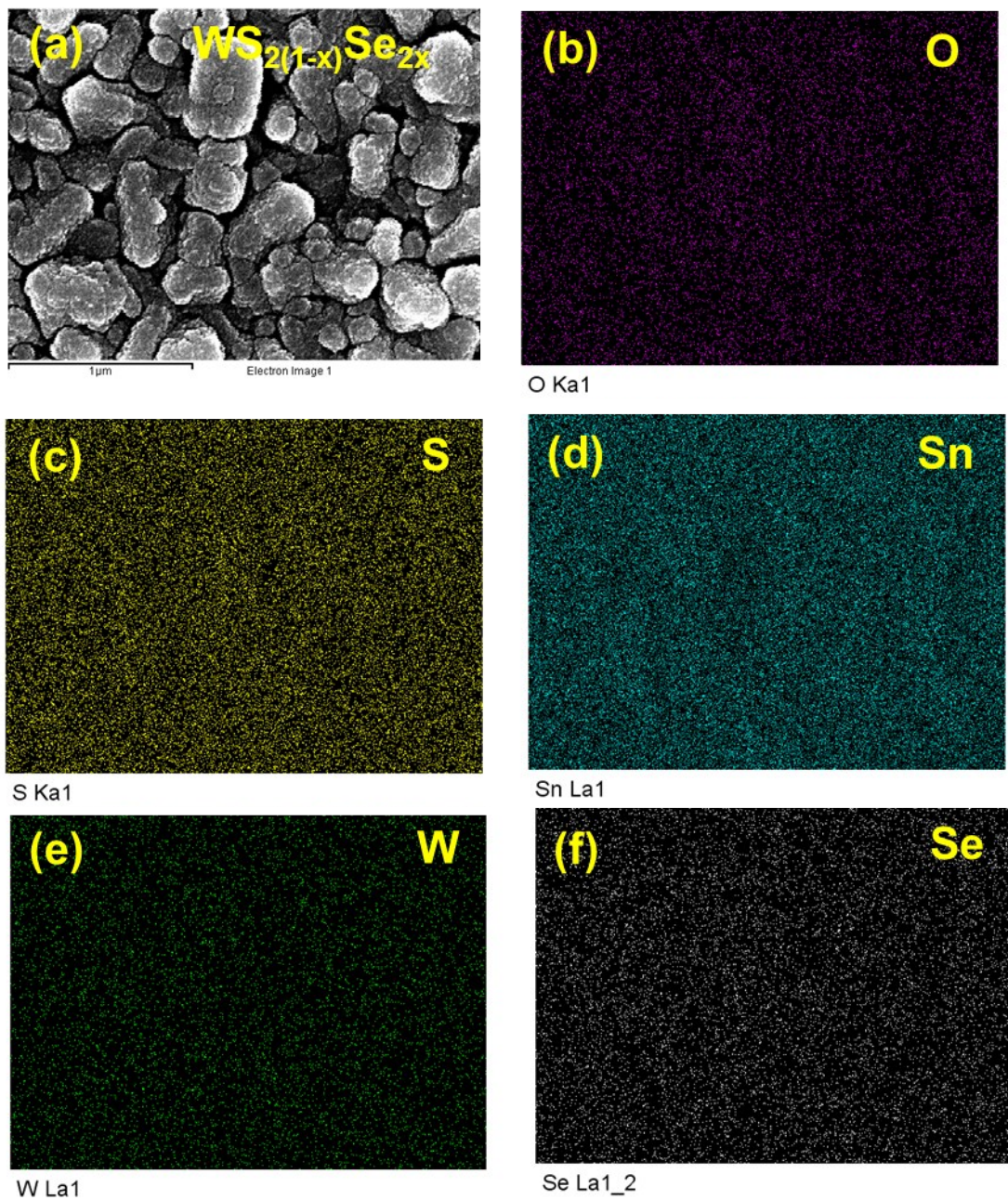


Figure S5. (a) FESEM image of $\text{WS}_{2(1-x)}\text{Se}_{2x}$ alloy and (b-f) their elemental mapping images (b) O, (c) Sn, (d) S, (e) W and (f) Se elements.

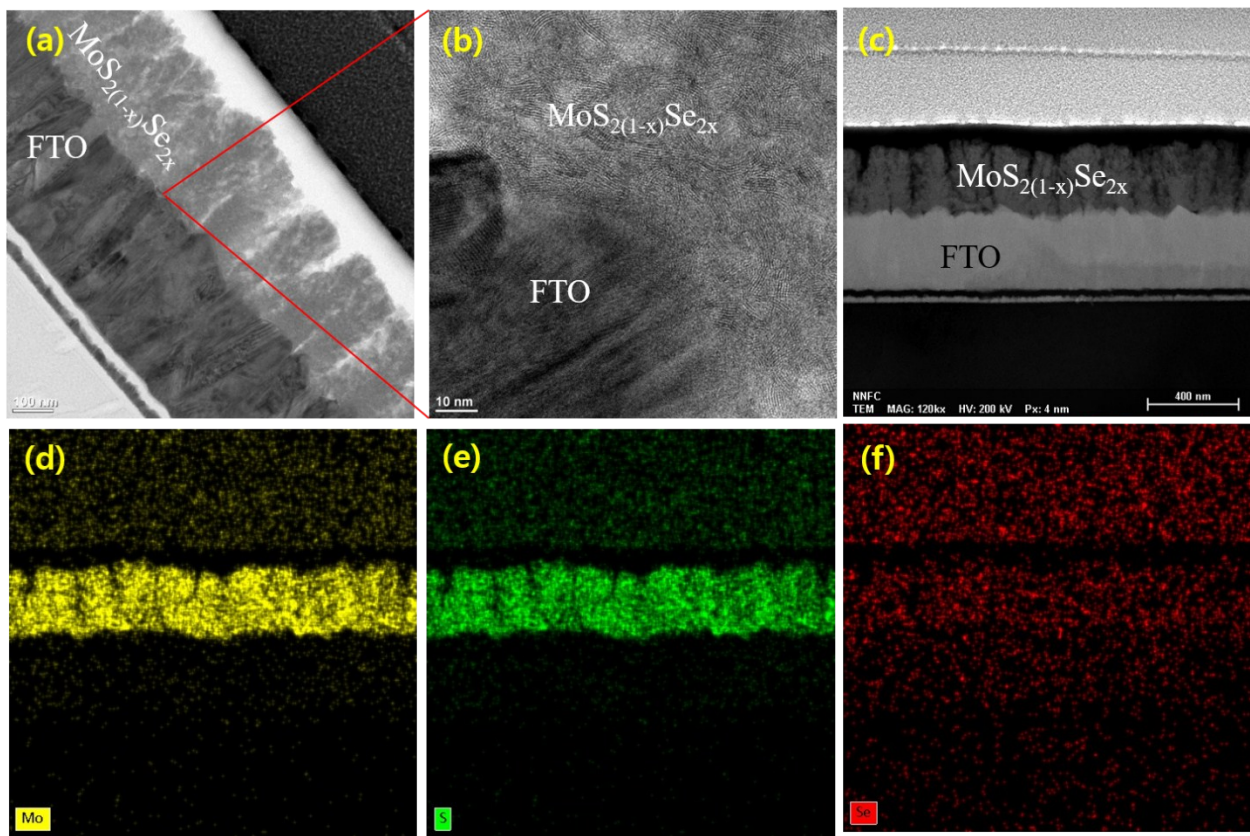


Figure S6. (a) TEM cross-sectional micrograph and (b) zoom-in view of FTO/MoS_{2(1-x)Se_{2x}} structure. (c-f) TEM cross-sectional micrograph and its elemental mapping images (d) Mo, (e) S and (f) Se elements for MoS_{2(1-x)Se_{2x}}.

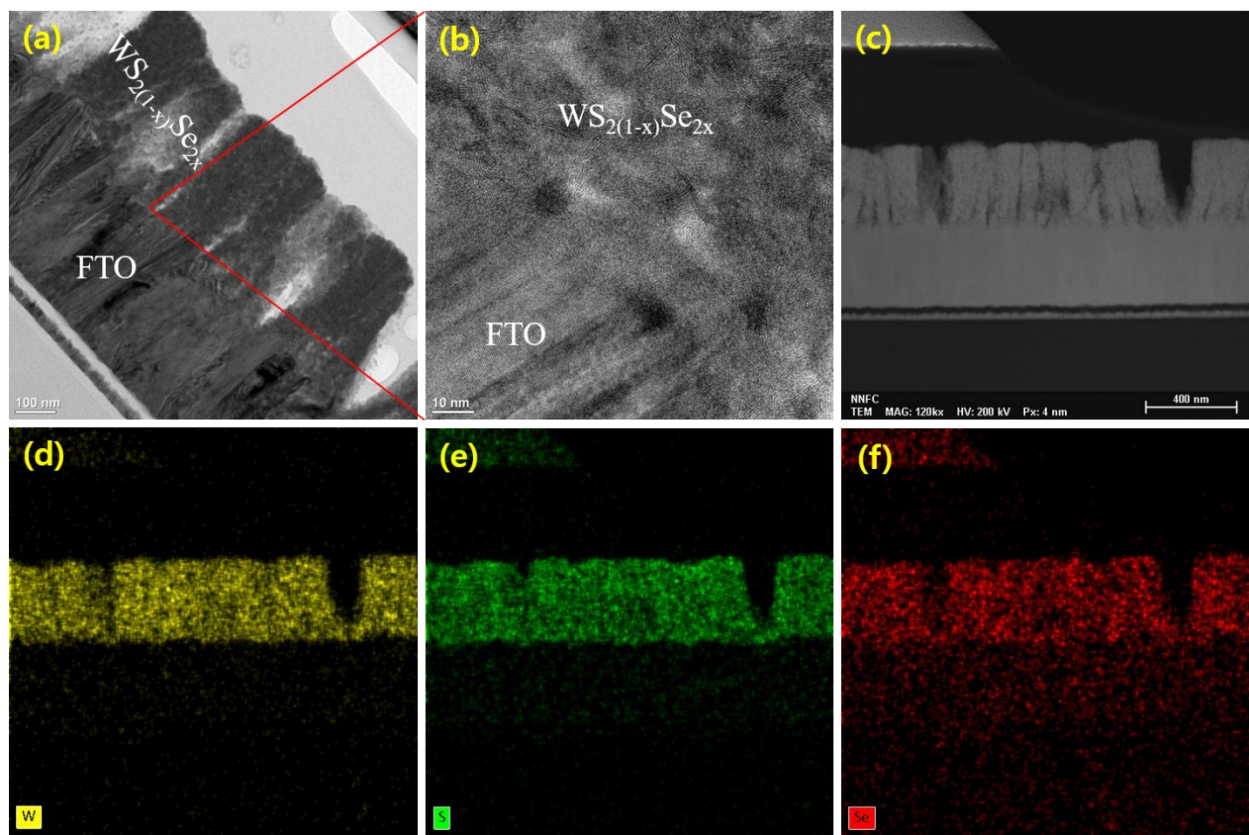


Figure S7. (a) TEM cross-sectional micrograph and (b) zoom-in view of FTO/WS_{2(1-x)}Se_{2x} structure. (c-f) TEM cross-sectional micrograph and its elemental mapping images (d) W, (e) S and (f) Se elements for WS_{2(1-x)}Se_{2x}.

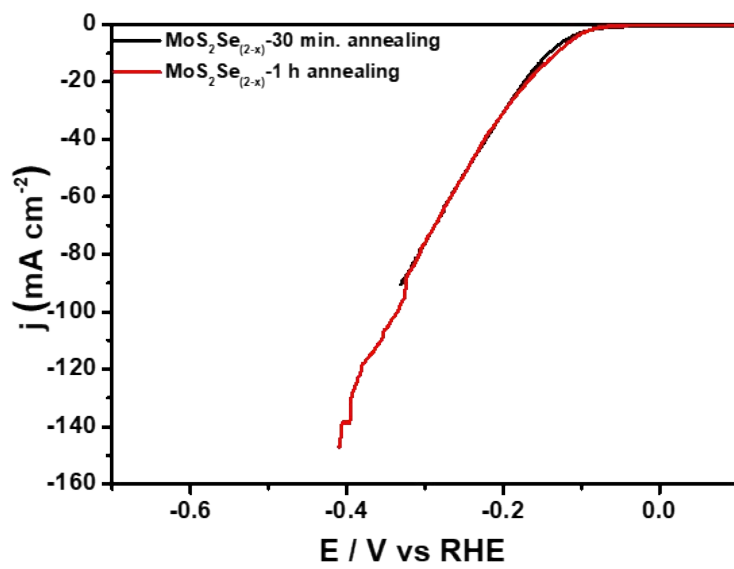


Figure S8. Polarization curves of $\text{MoS}_{2(1-x)}\text{Se}_{2x}$ film prepared using 30 min and 1 h post-annealing time in selenium environment at 500°C.

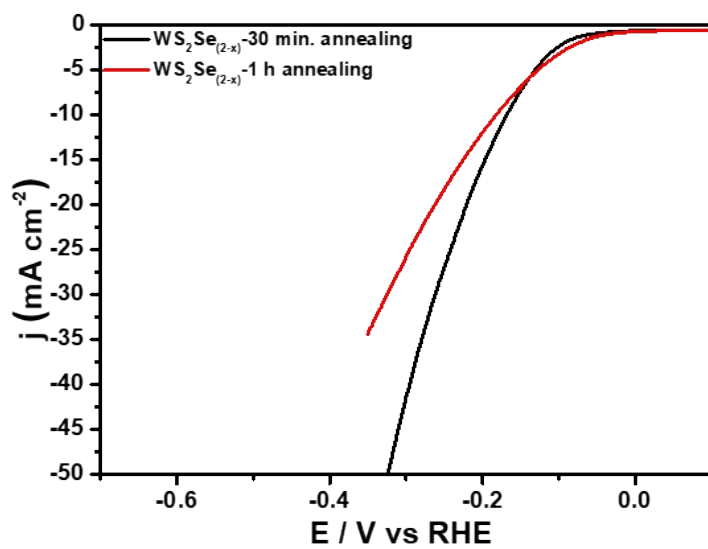


Figure S9. Polarization curves of $\text{WS}_{2(1-x)}\text{Se}_{2x}$ film prepared using 30 min and 1 h post-annealing time in selenium environment at 500°C.

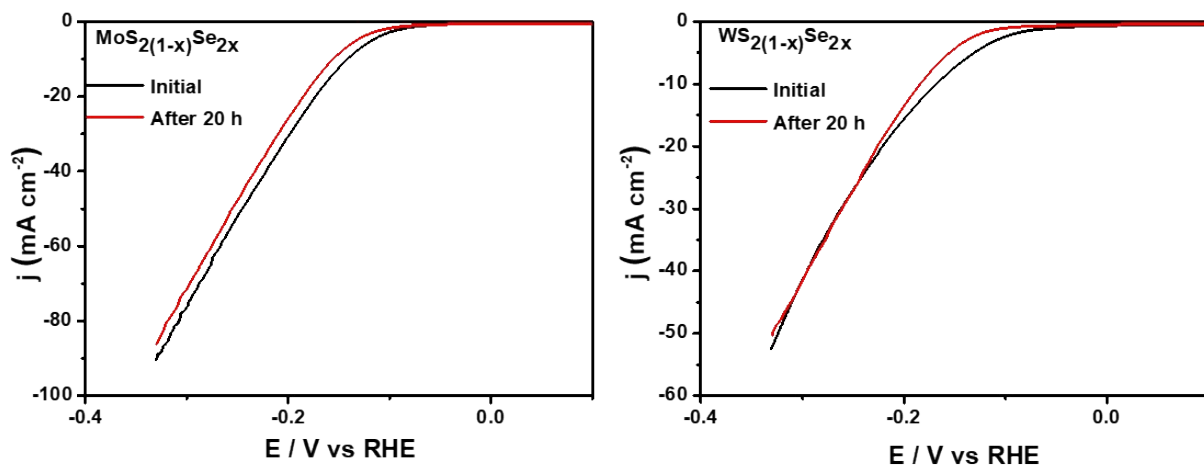


Figure S10. Stability test for $\text{MoS}_{2(1-x)}\text{Se}_{2x}$ and $\text{WS}_{2(1-x)}\text{Se}_{2x}$ alloy catalyst. **(a-b)** Polarization curves of $\text{MoS}_{2(1-x)}\text{Se}_{2x}$ and $\text{WS}_{2(1-x)}\text{Se}_{2x}$ alloy catalysts for before and after 20h HER performance.

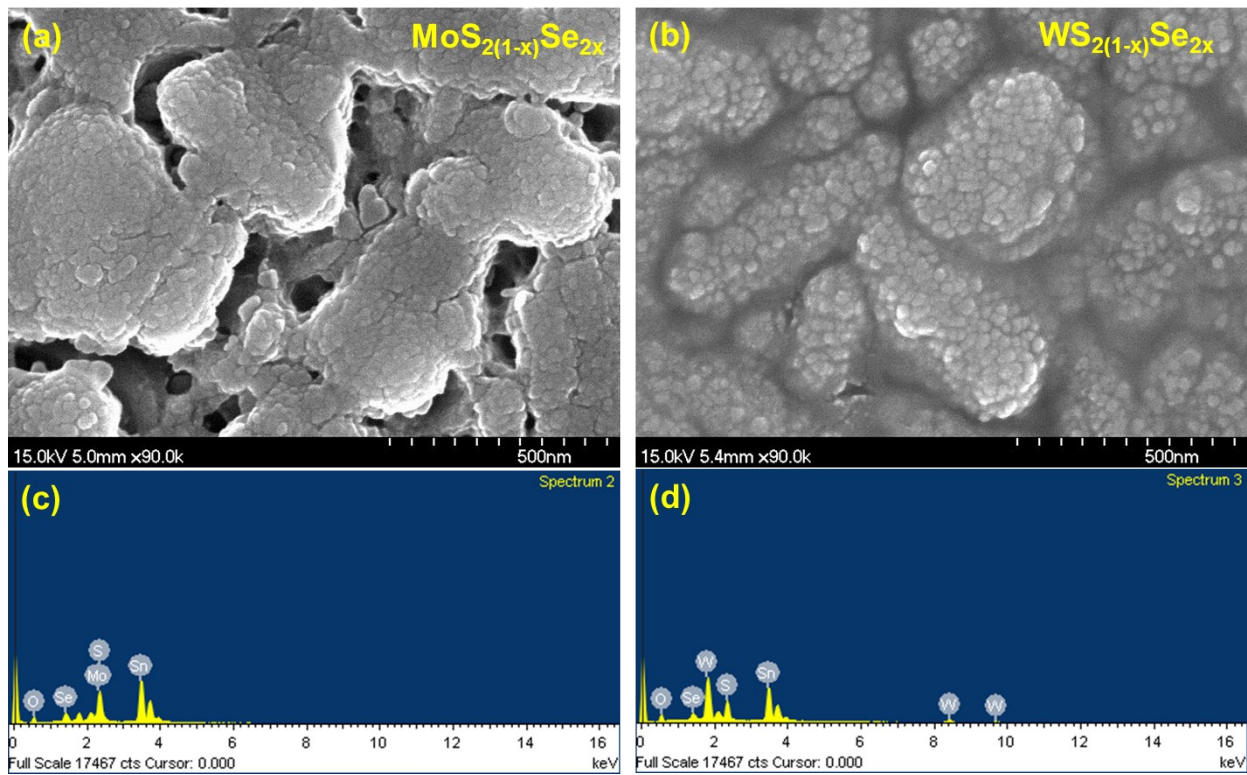


Figure S11. FE-SEM and EDS element analysis after 20 h HER operation. **(a, c)** $\text{MoS}_{2(1-x)}\text{Se}_{2x}$ and **(b, d)** $\text{WS}_{2(1-x)}\text{Se}_{2x}$ alloys.